CFD modelling of particle classification in mini-hydrocyclones

D. Vega-Garcia[a,*], J.J. Cilliers[b,], P. R. Brito-Parada[b,*]

[a]*Department of Metallurgical Engineering, University of Concepción, Concepción, Chile*
[b]*Department of Earth Science and Engineering, Imperial College London, London SW7 2AZ, UK*

Abstract

This work presents validated Computational Fluid Dynamics (CFD) predictions of the effect that changes in vortex finder and spigot diameters have on the classification performance of mini-hydrocyclones. Mini-hydrocyclones (e.g. 10 mm in diameter) have been applied successfully to the separation of micron-sized particles since their bypass fraction is larger than the water recovery, which results in a high particle recovery to the underflow, as well as low water recovery. However, a larger bypass fraction can be a disadvantage when the purpose of the hydrocyclone is particle classification, because of the large amount of fine particles that are misplaced in the underflow. Although it is well known that changes in the outlets of the hydrocyclone affect its performance, there is limited research on the effect of these design parameters in mini-hydrocyclones, in particular with regard to particle classification. The aim of this study is to computationally explore the influence of spigot and vortex finder on the classification process. To this end, CFD

*Corresponding authors
Email addresses: d.vega-garcia15@imperial.ac.uk (D. Vega-Garcia), p.brito-parada@imperial.ac.uk (P. R. Brito-Parada)

simulations were carried out and the predictions experimentally validated in a 3D printed mini-hydrocyclone using glass beads (below 20 µm) as the particulate system. The numerical results showed very good agreement with the experimental data for recovery of solids, concentration ratio, pressure drop and particle size distribution. A trade-off was observed between the solids recovery and concentration ratio, while the solids recovery was found to be inversely proportional to the pressure drop when vortex finder diameters were kept constant. It was found that the design that yielded the lowest recovery among those tested also resulted in a particle size distribution furthest away from that of the feed. We show how the model can be used to assess changes in design parameters in order to inform the selection of designs that exhibit lower energy requirements without compromising separation performance.
Keywords: mini-hydrocyclone, classification, 3D printing, modelling, CFD

1. Introduction

Mini-hydrocyclones are very effective for the separation of micron-sized particles because the cut sizes that hydrocyclones can achieve are directly proportional to their diameter. Thus, the application of mini-hydrocyclones for classification of particles has grown in popularity. It is generally accepted that in large hydrocyclones the bypass, i.e. the fraction of particles that reports to the underflow without classification, is normally equal to the water recovery. However, unlike large hydrocyclones, mini-hydrocyclones exhibit considerably larger bypass than the water recovery [1, 2, 3, 4]. This large bypass makes mini-hydrocyclones ideal for dewatering applications but poses a disadvantage for classification due to the amount of misplaced particles going to the underflow. While large hydrocyclones have been the subject of a vast amount of research (the reader is referred to a review on optimisation of geometric parameters by Ni et al. [5] and a review on the effect of operating parameters by Tian et al. [6]), there is still much work required to better understand mini-hydrocyclones. This is particularly relevant when the classification of fine and ultrafine particles is essential, such as in certain mineral processing, bioprocessing and pharmaceutical manufacturing applications.

Particle classification using mini-hydrocyclones has been the focus of some experimental studies. Abdollahzadeh et al. [7] showed that the classification efficiency in a 15mm hydrocyclone improves at low feed concentrations and high velocities, which is in agreement with the findings of Niazi et al. [2]. Pasquier and Cilliers [1] used experimental data to derive a semi-empirical model for the classification of fine silica in 10mm hydrocyclones. The effect of temperature and pressure on particle classification has also received attention in the literature. Cilliers et al. [3] demonstrated that an increase in temperature positively affects the recovery of fine silica particles in mini-hydrocyclones, by increasing the bypass and decreasing the cutsize, while Neesse et al. [8] reported that the cutsize in 10mm hydrocyclones can be further decreased by operating at higher pressures, which also trebled the throughput.

Design parameters also play a key role in the performance of hydrocyclones. Although the effect that changes in design parameters have on the separation efficiency of mini-hydrocyclones has been studied [9, 10], it is not fully understood. Experimental research on mini-hydrocyclone design parameters, such as spigot and vortex finder, has often been limited to designs that are commercially available. More recently, this drawback has been overcome by the application of 3D printing technology as a tool for manufacturing mini-hydrocyclones [11, 12, 13].

Numerical studies involving Computational Fluid Dynamics (CFD) simulations offer the possibility of exploring a wide range of changes in the design of mini-hydrocyclones. Ghodrat et al. [14] studied 75mm hydrocyclones using the Reynolds Stress Model (RSM) to calculate the turbulent flow field and applied the Multiphase Mixture model in FLUENT to simulate the fluid-particles system. In the Mixture model, unlike the Lagrangian-Eulerian model, the fluid and the solids are treated as interpenetrating continua and the interaction between the particles and fluid is considered. Ghodrat et al. [14] found that the performance of these hydrocyclones was affected more by the vortex finder diameter than by the vortex finder length. In a smaller, 55mm hydrocyclone, Yang et al. [15] carried out CFD simulations obtaining results close to their experimental data although overestimating the separation efficiency for very fine particles. They used the Renormalization Group (RNG) k - ϵ turbulence model for simulating the fluid and Lagrangian tracking for the particles. Even though the RNG turbulence model is more accurate than the standard k - ϵ model, for anisotropic turbulence and highly swirling flows, such as those found in hydrocyclones, the RSM model or Large Eddy Simulations (LES) can provide more accurate results [14, 16].

The effect of design parameters on the performance of small hydrocyclones, when considering the effect of changes in the particle size of the feed, has been the subject of numerical studies for 50 mm hydrocyclones. Zhang et al. [17] modelled the effect of changes in spigot diameter with fluctuations in the particle size distribution of the feed, finding that particle misplacement becomes important at small values of the spigot. A similar study but looking into the interactions between particle size variations and feed size distribution was carried out by Cui et al. [18].

A novel design was recently presented by Wang and Wu [19], who simulated two 45mm hydrocyclones using LES to calculate the flow field and the Lagrangian discrete phase model to track the particles. They compared a hydrocyclone with an overflow pipe to one with a tubular membrane. Wang and Wu [19] argued that the hydrocyclone with membrane reduces both the pressure drop in the system and the short-circuit of coarse particles to the overflow. Even though there was an improvement in the hydrocyclone performance, this was due to a modification in its structure but not to changes in the original design parameters. For smaller hydrocyclones (20 mm in diameter), Hwang et al. [20, 21] performed CFD simulations using the RSM turbulence model for the flow field and Lagrangian particle tracking for the trajectory of the solids. They demonstrated that by using a top plate with a cone angle of 30° and increasing the number of inlets, the performance of the hydrocyclones was improved. CFD analyses of even smaller, 10 mm hydrocyclones [22, 10, 11], have also been carried out, using the RSM turbulence model and validating the results against experimental data. However, there has been no comprehensive study on the effect of changes of both vortex finder and spigot diameters on particle classification. Shakeel Syed et al. [13] reported on the performance of 5 mm hydrocyclones with different outlet diameters but for a design with two tangential inlets and only considering two levels for the variables.

In this work, CFD simulations were carried out and were validated experimentally to predict the performance of 10mm mini-hydrocyclones for classification of particles. Experimental data was initially obtained from a 3D printed 10mm hydrocyclone with a spigot of 1 mm and a vortex finder of 2 mm and used for the validation of the CFD model. The CFD model was then used to further explore different designs of mini-hydrocyclones to understand the effect that changes in spigot and vortex finder have on hydrocyclone performance.

2. Methodology

The methodology of this work is divided into three steps: (i) CFD model set-up for a 10mm mini-hydrocyclone; (ii) experimental validation of the CFD model; and (iii) computational assessment of different designs. Four response parameters were taken into account to determine the performance of the mini-hydrocyclones evaluated:

- Recovery of solids, calculated as the mass of solids reporting to the underflow with respect to those present in the feed. It represents the total amount of solids being recovered in the underflow.

- Concentration ratio, defined as the underflow solids concentration divided by the feed solids concentration. It indicates how many times the feed is being concentrated in the underflow.

- The particle size distribution curve, which indicates the performance of the hydrocyclone for particles classification. The further the underflow curve is from the feed curve, the better the classification of the particles is. A characteristic number d(x) is the particle size that corresponds to the x% in the particle size distribution curve. It means that x% of the sample is smaller or equal to that particle size. The characteristic numbers most commonly used are d(20), d(50) and d(80).

- Pressure drop, a parameter related to the energy consumption needed to operate the hydrocyclone; smaller outlets in the hydrocyclones result in higher pressure drop for the same feed flow rate.

2.1. CFD model set-up

A numerical model was set-up in FLUENT 18 for the simulation of a mini-hydrocyclone with vortex finder 2 mm and spigot 1 mm, using a Eulerian-Lagrangian formulation (a valid approach for systems with volumetric concentrations of the disperse phase lower than 10% [23, 24, 25]). Water was defined as the continuous phase and soda lime glass as the disperse phase. Unstructured meshes with polyhedral elements, which were converted from tetrahedral elements, were used for transient simulations using adaptive time step. The adaptive time step was set with a truncation error tolerance of 0.01, a minimum and maximum time step size of $1\text{x}10^{-6}$ s and $1\text{x}10^{-3}$ s, respectively, and a maximum step change factor of 5. A mesh independence analysis was performed, for which meshes with different number of polyhedral elements, ranging from $1\text{x}10^5$ to $7.5\text{x}10^5$, were considered. Total pressure drop, underflow and overflow rates were used as reference for assessing convergence, from which the mesh with $2\text{x}10^5$ elements was selected for further simulations. In this work, the RSM turbulence model was selected as it has been shown to provide good predictions of flows in hydrocyclones at lower computational cost than LES simulations [26, 27]. RSM was used with a pressure-based solver and the Semi-Implicit Method for Pressure-Linked Equations (SIMPLE) algorithm for coupling pressure and velocity [28]. For the pressure discretization scheme, PRESTO was selected since this scheme is useful for predicting highly swirling flows [29]. A value of $1x10^{-4}$ was used as the convergence criterion for scaled residuals. In terms of boundary conditions, the inlet velocity was set to 15 ms^{-1}, corresponding to a feed flow of 60 mLs^{-1}, and the two outlets to atmospheric pressure, while no-slip boundary conditions were applied on the hydrocyclone walls. The wall-particle interaction was simulated in this work considering standard reflecting walls. On average the simulation time was 75 hours per hydrocyclone design.

After the continuous phase was solved, particles were injected using a Lagrangian discrete phase model. Ten injections of particles were created, with each injection corresponding to representative particle diameters. In this way, it possible to simulate more accurately the feed particle size distribution measured for the soda lime glass used for the experimental validation. For the particle force balance applied to the discrete phase, in addition to the drag force and gravity, other forces, such as pressure gradient and virtual mass forces, were included. These are forces required to accelerate the fluid surrounding the particle. The Discrete random walk model was applied to include the effect of instantaneous turbulent velocity fluctuations in the particle trajectories [30]. By using this model with a sufficient number of tries (i.e. representative particles), the random effects of turbulence on particle dispersion can be considered. Following a sensitivity analysis, the number of tries used in the simulations was 10, as this resulted in no incomplete particle tracks in the system, i.e. all the particles reported either to the underflow or the overflow. The injected particles were considered spherical, with a density of 2700 kgm^{-3} and an inlet velocity of 15 ms^{-1}, corresponding to the same velocity of the water. A total of 20800 parcels (the statistical representations of a number of individual particles) were injected into the hydrocyclone. These parcels accounted for the $2.7x10^{-4}$ kgs^{-1} injected in the feed. The simulated recovery of solids can be calculated as the particles reported to the underflow divided by the total particles injected.

2.2. Validation of the CFD model

2.2.1. Mini-hydrocyclone

The mini-hydrocyclone used for the experimental validation of the CFD model was 3D printed in an Objet30Pro printer using transparent acrylic material, which is able to withstand the pressure inside the hydrocyclone. The mini-hydrocyclone has a diameter of 10 mm, a cylindrical body height of 2 mm, a vortex finder length of 6 mm, vortex finder diameter of 2 mm, spigot diameter of 1 mm and a tangential square inlet of 4 mm^2 with a downward guided-channel. The conical section has a height of 51.4 mm, which provides a conic angle of 10°. The 3D printed mini-hydrocyclone was inserted in a housing, which was then connected to the piping system for the experiments. Figure 1 shows the 3D printed mini-hydrocyclone used for the experimental validation of the CFD model and a schematic diagram, with the dimensions given in millimetres.

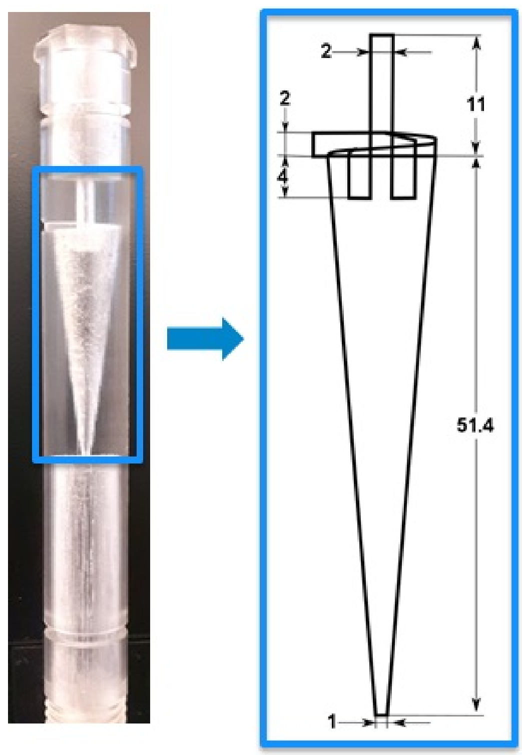

Figure 1: The 3D printed and a schematic diagram of the mini-hydrocyclone used for the experiments. Dimensions in the diagram are given in millimetres.

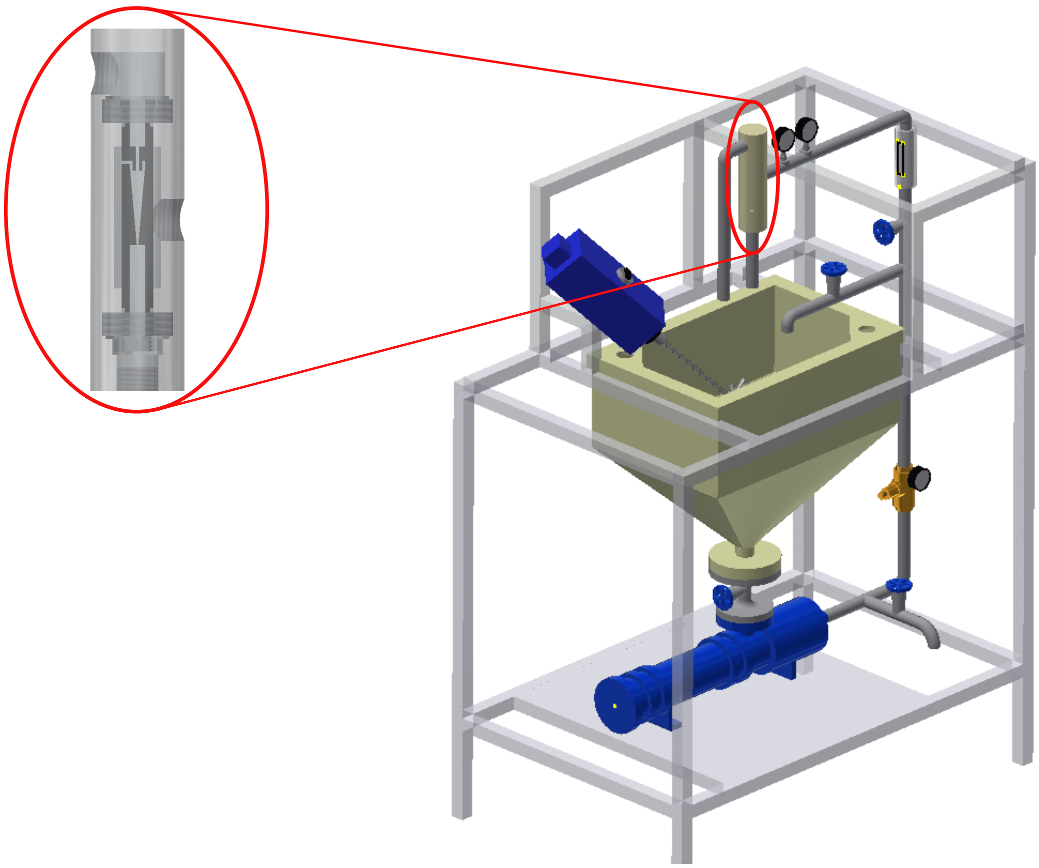

Figure 2: CAD model of the experimental rig. The mini-hydrocyclone is located inside a housing, which is connected to the piping system.

2.2.2. Experimental rig

The experimental rig consisted of a sump tank, positive displacement pump, flow control devices and the mini-hydrocyclone. Gauges for pressure and volumetric flow, as well as a pressure reducing valve to control the feed flow rate, were installed. A CAD model of the experimental rig used in the experiments is shown in Figure 2. The underflow and overflow discharged in the sump from a height that enabled direct sample collection. A schematic diagram and further details on the rig can be found in Vega-Garcia et al. [11].

2.2.3. Particulate system

The particulate system for the experiments was polished glass beads made of soda lime glass, which has a density of 2700 kgm^{-3}. Figure 3 shows the size distribution by mass and cumulative size distribution by mass of the particles. A narrow distribution can be observed, with a d_{10}=0.9 µm, d_{50}=4.5 µm and d_{90}=11.8 µm. The feed used for the experiments had a solids concentration of 4.5 gL^{-1} and a total flow rate of 60 mLs^{-1}.

2.2.4. Experimental procedure

The stirrer was turned on before the suspension of solids were added into the water in the sump tank to avoid agglomeration of the particles. After the suspension was homogenized, the pump was turned on and the valves adjusted until the flow through the mini-hydrocyclone reached 60 mLs^{-1}. Once the desired flow was obtained, the system was left to run for 1 minute until

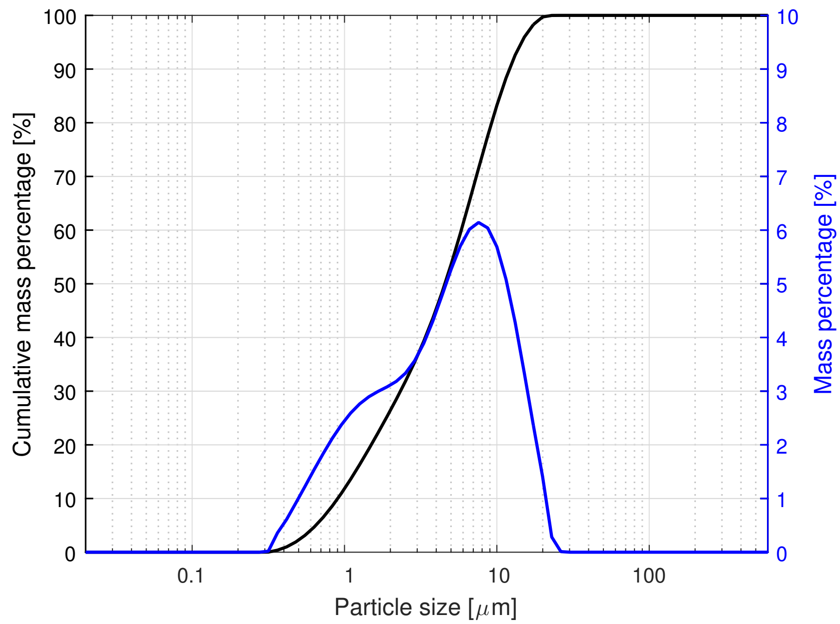

Figure 3: Cumulative and individual size distribution of the particles used in the experimental work. Average values based on three samples of the feed material are reported (standard deviation was insignificant and thus not reported).

steady state was reached. In order to determine the flow rates, timed samples were taken from the underflow and overflow simultaneously. To calculate the solids concentration, samples from the feed, underflow and overflow were collected and dried. Additional samples were taken and directly analyzed for particle size distribution (PSD) in a Malvern Mastersizer 3000. The PSD analysis was done without drying the samples to avoid agglomeration of particles. Determination of flow rates, solids concentrations and PSD were carried out in triplicate to ensure repeatability.

2.3. Exploration of new designs computationally

2.3.1. Full factorial design

A full factorial design, considering three values of vortex finder and four values of spigot was used for the simulations in this work. Vortex finder diameters (VF) of 3.2, 2.6 and 2.0 mm, and spigot diameters (S) of 2.5, 2.0, 1.5 and 1.0 mm, were evaluated. It is important to mention that the rest of the design variables were kept constant and that the CFD simulations for all the mini-hydrocyclones were run under the same operating conditions and model parameters.

3. Results and discussion

3.1. CFD model results and validation

The CFD model for the mini-hydrocyclone VF2 S1 was run under the conditions described in Section 2. The 3D printed mini-hydrocyclone was run in the experimental rig under the same design and operating conditions as in the CFD simulation. Table 1 shows the simulated and experimental results for solids recovery, concentration ratio and pressure drop. The results show that the performance of the mini-hydrocyclone predicted by the model exhibits errors below 10%. The larger error in the concentration ratio is likely due to an error propagation from the prediction of the underflow; a small difference in the flow rates generates a more significant difference in the solids concentration and, in turn, in the concentration ratio.

Table 1: Comparison between CFD simulated and experimental results for the VF2 S1 mini-hydrocyclone. The experimental data is reported with standard deviation and the error between the CFD and experimental data is provided.

Response parameter [-]	**CFD**	**Experimental**	**Error** [%]
Solids recovery [%]	75.1	71.13 ±0.26	5.6
Concentration ratio [-]	4.6	5.12 ±0.01	9.5
Pressure drop [kPa]	735	800 ±23	8.1

A comparison of the simulated and experimental PSD of the mini-hydrocyclone VF2 S1 underflow is shown in Figure 4. For the experimental data, three samples were taken and each one analysed using the Malvern MasterSizer 3000, in which five measurements were taken per sample; data showed extremely low variability and the particle size distribution is thus shown as a continuous line. It can be seen that there is a very good agreement between the simulated and experimental results. The model predicts very well the solids recovery and particle size distribution, two very important parameters in classification of particles, which is the focus of this work.

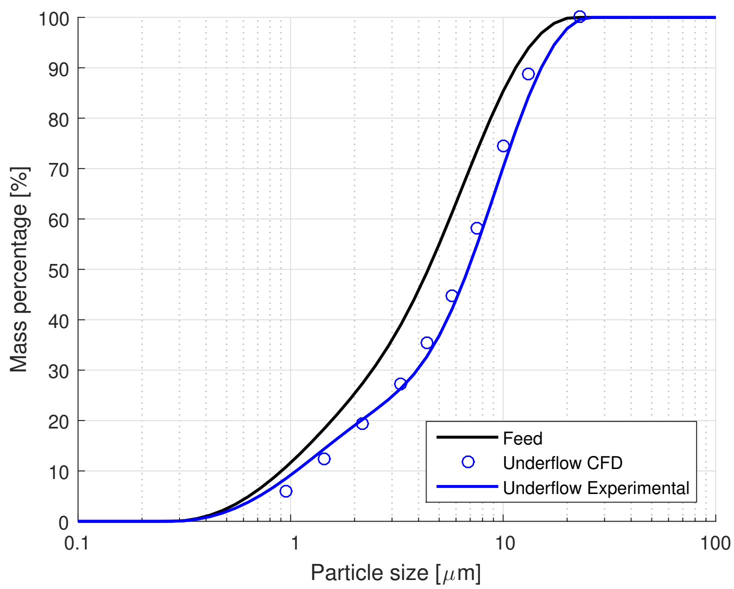

Figure 4: Particle size distribution of the underflow of the mini-hydrocyclone VF2 S1. A very good agreement between the simulated and experimental results is observed. The experimental Particle Size Distribution data are shown as continuous lines, as values from repeats fall on top of each other

.

3.2. Assessment of new designs computationally

3.2.1. Solids recovery and Concentration ratio

As mentioned before, a series of mini-hydrocyclones with combination of vortex finders (VF) 2, 2.6 and 3.2 mm and spigots (S) 1, 1.5, 2 and 2.5 mm were simulated. The results for the mini-hydrocyclone VF3.2 S1 are not shown because the predicted underflow rate value obtained was negligible. The simulated values of recovery of solids and concentration ratio are summarized in Figure 5, where a trade-off between these variables is observed, with the hydrocyclones achieving high values of concentration ratio at the expense of low recovery of solids, and vice versa. Also, when vortex finders are kept constant and the spigot diameter decreases, the recovery of solids decreases while concentration ratios increase. This is attributed to the fact that a smaller spigot diameter creates higher pressure in the system (see Figure 8, discussed later in Section 3.3), which improves the separation of particles and the concentration effect. However, a smaller spigot diameter results in a reduction of the underflow flow rate, thus lowering the solids recovery that can be achieved. The same trend is observed for the three sets of mini-hydrocyclones (i.e. those with vortex finders 3.2, 2.6 and 2.0 mm).

The set of mini-hydrocyclones with vortex finder 2 mm shows a slightly better performance in solids recovery than the set with vortex finder 2.6 mm, although the latter achieves considerably higher concentration ratio values when the spigot diameter is 1 mm. The mini-hydrocyclones with vortex finder 3.2 mm achieve smaller solids concentration but higher concentration ratios than their counterparts for similar spigot diameters.

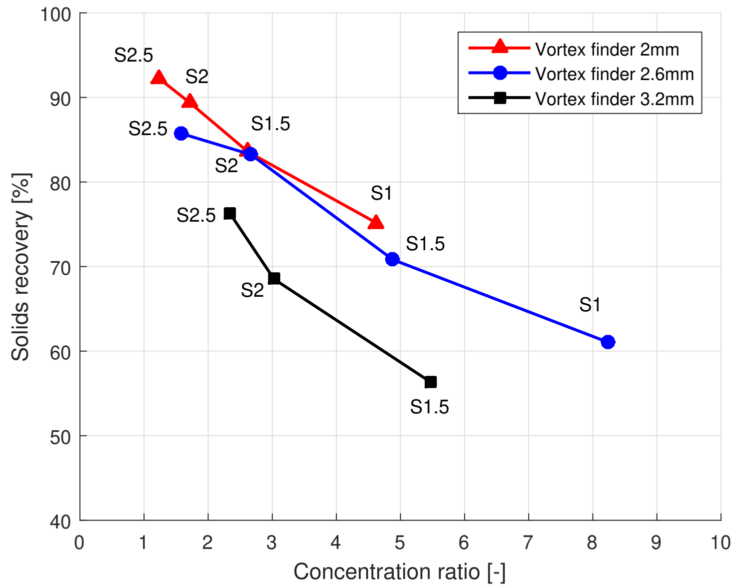

Figure 5: CFD results of solids recovery and concentration ratio in mini-hydrocyclones: a trade-off between these variables is observed.

3.2.2. Particle size distribution

The CFD model was used to simulate the particle size distribution (PSD) curves for all the mini-hydrocyclones considered in the full factorial design. Figure 6 shows the simulated underflow particle size distribution curves for the mini-hydrocyclones. It can be seen that changes in design generate differences in the PSD of the underflow. There is a wide distribution of the underflow PSDs, with some of these overlapping one another. It is observed that the PSD of the mini-hydrocyclone VF2 S2.5 is the closest to the feed curve, showing poor classification after the material passes through the mini-hydrocyclone, while the PSD of design VF3.2 S1.5 is the one that is furthest away from the feed, yielding the coarsest particle distribution of them all. Interestingly, these results correspond to the mini-hydrocyclones with highest and lowest solids recovery, respectively (see Figure 5). In the mini-hydrocyclone VF2 S2.5 most of the particles that were injected report to the underflow, and there is therefore no significant difference between the feed and the underflow size distribution. On the other hand, due to the lowest solids recovery achieved by the mini-hydrocyclone VF3.2 S1.5, more fine particles report to the overflow, turning the underflow into a stream with a coarser PSD. A summary of the characteristic numbers for all the particle size distribution curves is presented in Table 2.

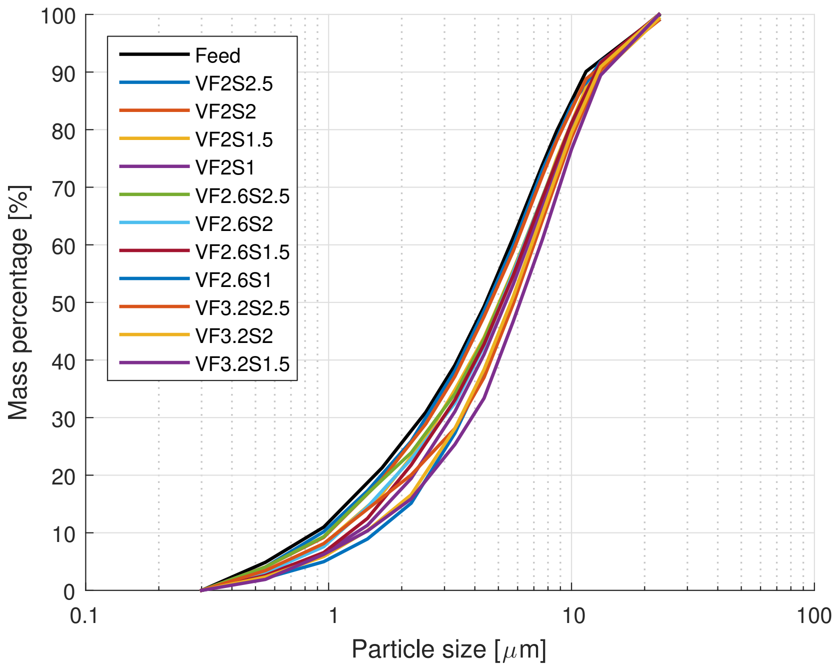

Figure 6: Particle size distribution in the underflows of the simulated mini-hydrocyclones.

Table 2: Characteristic numbers for all the PSD curves simulated. All the values are given in millimetres.

Mini-hydrocyclone	**d(20)**	**d(50)**	**d(80)**
VF2 S2.5	1.68	4.54	9.10
VF2 S2	1.72	4.67	9.19
VF2 S1.5	1.94	5.09	9.82
VF2 S1	2.24	5.40	9.93
VF2.6 S2.5	1.78	5.12	9.79
VF2.6 S2	1.93	5.19	9.79
VF2.6 S1.5	2.04	5.21	9.79
VF2.6 S1	2.64	5.67	10.2
VF3.2 S2.5	2.18	5.79	10.4
VF3.2 S2	2.52	5.64	10.1
VF3.2 S1.5	2.68	6.18	10.9

3.3. Mini-hydrocyclone design selection informed by CFD

This section describes the application of the CFD model for the selection of a mini-hydrocyclone design. As can be seen in Figure 5, the hydrocyclones VF2 S1.5 and VF2.6 S2 show the same performance, with values for solids recovery and concentration ratio of approximately 83% and 2.6, respectively. Another comparison between these two designs, but for a different response parameter, particle size distribution, can bee seen in Figure 7; interestingly, particle size distribution curves for both mini-hydrocyclones are very similar. Up to this point, the similarity between these two designs has been shown for the behaviour of particles, which determines classification performance. However, further details can be obtained from the CFD simulations, such as the pressure drop and the velocities for each mini-hydrocyclone design.

3.3.1. Pressure drop

A summary of the simulated total pressure drops for all the mini-hydrocyclones is shown in Figure 8. It is observed that when the spigot diameter remains constant, an increase in vortex finder generates higher pressure drops. Similarly, when the spigot diameter is reduced at a constant vortex finder diameter, the pressure in the system increases. This effect is more pronounced in the set of mini-hydrocyclones with vortex finder 2 mm, which is expected as they already have smaller vortex finders in comparison to the other mini-hydrocyclones. Figure 8 also shows that the pressure drops in the mini-hydrocyclones are inversely proportional to their corresponding solids recoveries (Figure 5). The same effect is observed in the three groups of mini-hydrocyclones with different vortex finder. In addition, Figure 9

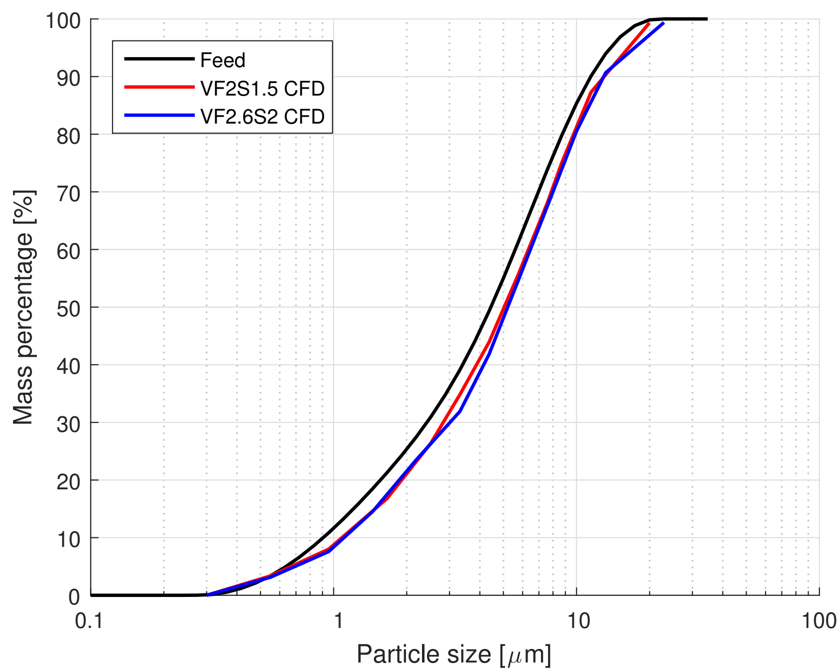

Figure 7: Comparison of the simulated underflow particle size distributions of the mini-hydrocyclones VF2 S1.5 and VF2.6 S2

shows the cross-sectional total pressure distribution for all the simulated mini-hydrocyclones. It can be observed that the low pressure zones are present in all the cases and that they are approximately the same width as the spigot diameter.

From Figure 8 and Figure 9 it can be observed that the pressure drops in mini-hydrocyclones VF2 S1.5 and VF2.6 S2 are different, despite these designs resulting in the same particle behaviour. The mini-hydrocyclone VF2.6 S2 can therefore be selected over VF2 S1.5, in order to achieve the same performance at lower energy consumption. This highlights how a mini-hydrocyclone design for a particular task can be selected, taking into account as much information about the performance as possible.

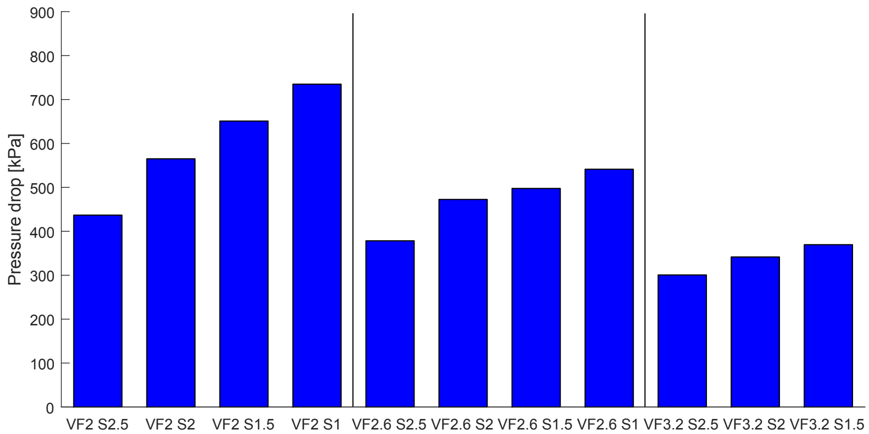

Figure 8: Summary of the simulated pressure drop for all the designs, displayed in groups of mini-hydrocyclones with the same vortex finder diameter.

3.3.2. Velocities

The CFD results for the velocities inside the different mini-hydrocyclone designs can also be used to better understand performance. Axial, radial and tangential velocities for all the designs considered in this work are shown in Figures S1, S2 and S3, respectively, in the Supplementary Material. In particular, higher axial velocities near the spigot and vortex finder can be linked to higher pressure drops, which is consistent with the fact that VF2.6 S2 has lower energy requirements than VF2 S1.5. As can be seen in Figure S1, the latter presents higher velocities near the outlets. Similarly, high tangential velocities near the vortex finder can be observed in Figure S3 for VF2 S1.5; this is in fact the case for a given vortex finder diameter as the diameter of the spigot decreases, and is particularly noticeable at the lowest vortex finder values tested. While clearly the velocity profiles in the mini-

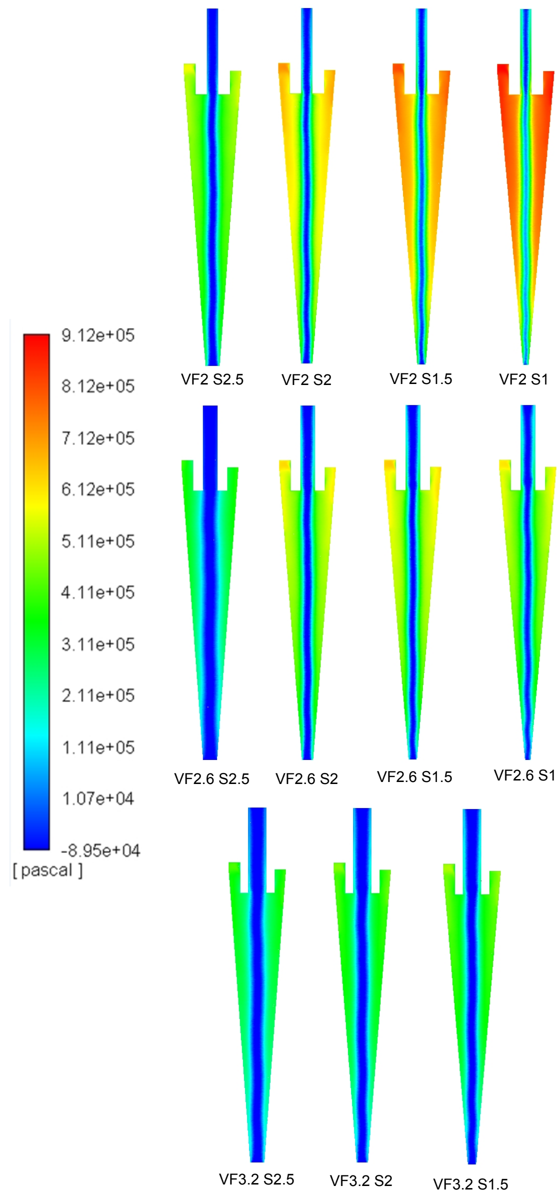

Figure 9: Cross-sectional total pressure distribution for all the mini-hydrocyclones simulated.

hydrocyclones cannot be directly linked to the recovery and concentration ratio that a given design yields, the aforementioned features are linked to pressure requirements and thus impact overall performance.

3.3.3. Further validation of the CFD model

An experimental verification of the predicted results obtained for the mini-hydrocyclones VF2 S1.5 and VF2.6 S2 was performed. These designs were 3D printed and then experiments were carried out under the same operating conditions as the CFD simulations. A comparison between the numerical and experimental results is shown in Table 3. It can be observed that there is only a small difference between the CFD and experimental results, in particular for solids recovery, for which errors are below 5%. It is also important to note that the experimental results for solids recovery and concentration ratio for the mini-hydrocyclones VF2 S1.5 and VF2.6 S2 are very similar, as predicted by the CFD simulation results.

Finally, also similar to what is predicted by the simulations, the pressure drop obtained in the mini-hydrocyclone VF2 S1.5 is larger than that in the mini-hydrocyclone VF2.6 S2. This confirms that the CFD model presented in this work can accurately predict the behaviour of relevant operating variables for particle classification in mini-hydrocyclones with a range of outlet diameters.

4. Conclusions

An Eulerian-Lagrangian CFD model was used to understand the effect that changes in vortex finder and spigot diameters have on particle classification in mini-hydrocyclones. This CFD model was validated with experiments performed in 3D printed mini-hydrocyclones. Good agreement was found

Table 3: Comparison between CFD simulated and experimental results for the VF2 S1.5 and VF2.6 S2 mini-hydrocyclones. The experimental data is reported with standard deviation and the error between the CFD and experimental data is provided.

Response parameter [-]	**CFD**	**Experimental**	**Error** [%]
Solids recovery VF2 S1.5 [%]	83.4	79.4 ±0.54	4.8
Solids recovery VF2.6 S2 [%]	83.2	79.3 ±2.36	4.7
Concentration ratio VF2 S1.5 [-]	2.62	2.27 ±0.01	13.3
Concentration ratio VF2.6 S2 [-]	2.67	2.55 ±0.19	4.5
Pressure drop VF2 S1.5 [kPa]	651	600 ±12	7.8
Pressure drop VF2.6 S2 [kPa]	473	430 ±10	9.1

between the predicted and experimental results for the evaluated response parameters, i.e. recovery of solids, concentration ratio, pressure drop and particle size distribution results.

Three different vortex finders and four different spigots were evaluated computationally through a full factorial design in order to assess the interactions among the response parameters. In particular, a trade-off was observed between the solids recovery and concentration ratio, while the solids recovery was found to be inversely proportional to the pressure drop, when vortex finder diameters were kept constant. The particle size distributions for the different designs were also analysed and showed to be linked to solids recovery.

This works shows how the information obtained through CFD modelling can be used to assess response parameters and inform the selection of mini-hydrocyclone designs that result in lower pressure drop without impacting the classification performance. This has important implications for the reduction in energy consumption in mini-hydrocyclones and can thus lead to more efficient classification systems for micron-sized particles.

Acknowledgement

This research was carried out as part of PRODIAS, a project funded by the European Community's Framework Programme for Research and Innovation Horizon 2020 (2014-2020) under grant agreement no. 637077.

References

[1] S. Pasquier, J. J. Cilliers, Sub-micron particle dewatering using hydrocyclones, Chemical Engineering Journal 80 (2000) 283–288.

[2] S. Niazi, M. Habibian, M. Rahimi, A Comparative Study on the Separation of Different-Shape Particles Using a Mini-Hydrocyclone, Chemical Engineering and Technology 40 (2017) 699–708.

[3] J. J. Cilliers, L. Diaz-Anadon, F. S. Wee, Temperature, classification and dewatering in 10 mm hydrocyclones, Minerals Engineering 17 (2004) 591–597.

[4] W. Kraipech, W. Chen, F. J. Parma, T. Dyakowski, Modelling the fishhook effect of the flow within hydrocyclones, International Journal of Mineral Processing 66 (2002) 49–65.

[5] L. Ni, J. Tian, T. Song, Y. Jong, J. Zhao, Optimizing geometric parameters in hydrocyclones for enhanced separations: A review and perspective, Separation and Purification Reviews 48 (2019) 30–51. Cited By 14.

[6] J. Tian, L. Ni, T. Song, J. Olson, J. Zhao, An overview of operating parameters and conditions in hydrocyclones for enhanced separations, Separation and Purification Technology 206 (2018) 268 – 285.

[7] L. Abdollahzadeh, M. Habibian, R. Etezazian, S. Naseri, Study of particle's shape factor, inlet velocity and feed concentration on mini-hydrocyclone classification and fishhook effect, Powder Technology 283 (2015) 294–301.

[8] T. Neesse, J. Dueck, H. Schwemmer, M. Farghaly, Using a high pressure hydrocyclone for solids classification in the submicron range, Minerals Engineering 71 (2015) 85–88.

[9] L. R. Castilho, R. A. Medronho, Simple procedure for design and performance prediction of Bradley and Rietema hydrocyclones, Minerals Engineering 13 (2000) 183–191.

[10] K.-J. Hwang, S.-P. Chou, Designing vortex finder structure for improving the particle separation efficiency of a hydrocyclone, Separation and Purification Technology 172 (2017) 76–84.

[11] D. Vega-Garcia, P. R. Brito-Parada, J. J. Cilliers, Optimising small hydrocyclone design using 3D printing and CFD simulations, Chemical Engineering Journal 350 (2018) 653–659.

[12] P. R. Brito-Parada, R. M. Dewes, D. Vega-Garcia, J. J. Cilliers, Influence of Design Parameters on Biomass Separation in Mini-hydrocyclones, Chemical Engineering & Technology (2018) 1–9.

[13] M. Shakeel Syed, M. Rafeie, R. Henderson, D. Vandamme, M. Asadnia, M. Ebrahimi Warkiani, A 3D-printed mini-hydrocyclone for high throughput particle separation: application to primary harvesting of microalgae, Lab Chip 17 (2017) 2459–2469.

[14] M. Ghodrat, S. B. Kuang, A. B. Yu, A. Vince, G. D. Barnett, P. J. Barnett, Numerical analysis of hydrocyclones with different vortex finder configurations, Minerals Engineering 63 (2014) 125–138.

[15] I. H. Yang, C. B. Shin, T. Kim, S. Kim, A three-dimensional simulation of a hydrocyclone for the sludge separation in water purifying plants and comparison with experimental data, Minerals Engineering 17 (2004) 637–641.

[16] J. A. Delgadillo, R. K. Rajamani, A comparative study of three turbulence-closure models for the hydrocyclone problem, International Journal of Mineral Processing 77 (2005) 217–230.

[17] C. Zhang, B. Cui, D. Wei, S. Lu, Effects of underflow orifice diameter on the hydrocyclone separation performance with different feed size distributions, Powder Technology 355 (2019) 481 – 494.

[18] B. Cui, C. Zhang, D. Wei, S. Lu, Y. Feng, Effects of feed size distribution on separation performance of hydrocyclones with different vortex finder diameters, Powder Technology 322 (2017) 114 – 123.

[19] C. C. Wang, R. M. Wu, Experimental and simulation of a novel hydrocyclone-tubular membrane as overflow pipe, Separation and Purification Technology 198 (2018) 60–67.

[20] K. J. Hwang, Y. W. Hwang, H. Yoshida, K. Shigemori, Improvement of particle separation efficiency by installing conical top-plate in hydrocyclone, Powder Technology 232 (2012) 41–48.

[21] K.-J. Hwang, Y.-W. Hwang, H. Yoshida, Design of novel hydrocyclone for improving fine particle separation using computational fluid dynamics, Chemical Engineering Science 85 (2013) 62–68.

[22] S. Grady, G. Wesson, M. Abdullah, E. Kalu, Prediction of 10-mm Hydrocyclone Separation Efficiency Using Computational Fluid Dynamics, Filtration & Separation 40 (2003) 41–46.

[23] R. Safa, A. Soltani Goharrizi, CFD simulation of an industrial hydrocyclone with Eulerian-Eulerian approach: A case study, International Journal of Mining Science and Technology 24 (2014) 643–648.

[24] S. Swain, S. Mohanty, A 3-dimensional Eulerian-Eulerian CFD simulation of a hydrocyclone, Applied Mathematical Modelling 37 (2013) 2921–2932.

[25] S. B. Kuang, K. W. Chu, A. B. Yu, A. Vince, Numerical study of liquid-gas-solid flow in classifying hydrocyclones: Effect of feed solids concentration, Minerals Engineering 31 (2012) 17–31.

[26] M. Narasimha, M. Brennan, P. N. Holtham, A review of CFD modelling for performance predictions of hydrocyclone, Engineering Applications of Computational Fluid Mechanics 1 (2007) 109–125.

[27] M. Ghodrat, Z. Qi, S. B. Kuang, L. Ji, A. B. Yu, Computational investigation of the effect of particle density on the multiphase flows and performance of hydrocyclone, Minerals Engineering 90 (2015) 55–69.

[28] J. P. Van Doormaal, G. D. Raithby, Enhancements of the simple method for predicting incompressible fluid flows, Numerical Heat Transfer 7 (1984) 147–163.

[29] K. U. Bhaskar, Y. R. Murthy, N. Ramakrishnan, J. K. Srivastava,

S. Sarkar, V. Kumar, CFD validation for flyash particle classification in hydrocyclones, Minerals Engineering 20 (2007) 290–302.

[30] A. D. Gosman, E. Ioannide, Aspects of computer simulation of liquid-fuelled combustors, Journal of Energy 7 (1983) 482–490.